EXACT TWO-DIMENSIONAL RECTANGULAR FIN SOLUTION VERSUS IMPROVED CLASSICAL ONE-DIMENSIONAL RADIAL FIN WITH APPLICATION IN ELECTRICAL ENGINE

Élcio Nogueira
Department of Mechanics and Energy – DME/FAT / UERJ - Resende - RJ – Brazil
elcionogueira@hotmail.com

ABSTRACT

Extended surfaces are widely used in engineering applications for greater efficiency in heat transfer rate. Indeed, extended surfaces are of great importance in the design of heat exchange devices in different fields of application in order to provide an improved heat transfer effect through an increase in the total heat exchange area. Among the various possible applications in engineer, the design of cooling systems for electronic devices with extended surfaces, such as in modern computers, requires highly optimized configurations, predictive and precise mathematical analyses. Exact analytical solution of two-dimensional, steady-state heat conduction in an extending rectangular surface is presented. A polynomial interpolation was developed for Modified Bessel Functions, in all ranges of applicability. In addition, the improved classic one-dimensional model for radial fins is critically examined for this type of profile. The influence of governing parameters, Biot number and aspect ratio, is investigated and comparison is made in relation of results of literature. Results for efficiency and effectiveness, depending on the Biot number and aspect ratio as a parameter, are presented. Applications for extended surfaces in electric motors are also analyzed, because of their vital importance in the industry since they are extensively used in machines of all types.

KEYWORDS: *Extend surfaces; Rectangular Fin; Radial Fin; Finned Electric Motor*

I. INTRODUCTION

Fins or extended surfaces are extensively used in engineering applications to increase the heat transfer efficiency of surfaces. In fact, extended surfaces are of vital importance in the design of heat exchange devices in different fields of application in order to provide an enhanced heat transfer effect through an increase in the total heat exchange area. Once the temperature distribution through the fin is known, the heat transfer rate and the efficiency, or effectiveness, can be readily determined. Among the various possible applications in engineering of extended surfaces, the design of cooling systems for electronic devices, such as in modern computers, requires highly optimized configurations and precise predictive mathematical analyses A.D. Kraus (1993), S. Oktay (1993), R.M. Cotta, R. Ramos (1993).

Cotta and Mikhailov (1997) presented a general hybrid numerical-analytical solution for longitudinal fins with arbitrarily variable profile and temperature dependent thermal conductivity, associated to steady-state two-dimensional heat conduction problem. They used the Generalized Integral Transform Technique - GITT of previous development on diffusion and convection within irregular geometries, including the nonlinear nature introduced through the variable thermal conductivity.

Recently, Antonio Campo and Balaram Kundu (2017) presented an exact analytical model to determine temperature distributions, heat transfer rates and fin efficiencies for annular fins. The two-dimensional heat conduction equations applied to annular fins are solved with modified Bessel functions of first and second order type zero and one. Concise correlation equations for the calculation of fin efficiency and uniform thickness tip temperature were developed.

An exact solution using Laplace transform is developed by George Oguntalaa et al. (2019). They analyze the effects of the convective tip on the theoretical predictions of solid fin thermal performance, and conclude that increasing the Biot number in the convective, radiative, and magnetic variables improves fin efficiency.
Karinate Valentine Okiy (2015) considered two-dimensional temperature distributions in different fins configurations (radial rectangular fins, planar rectangular fins) in contrast to the one-dimensional assumption commonly used in most design methodologies. She found that the one-dimensional approach does not always give good results for heat fluxes and temperature distributions for the flat and radial rectangular fins, but she does not analyze the aspect ratio and does not include comparative studies for the wide range of Biot numbers.

Juca and Prata argue that the inclusion of two-dimensional effects to consider the non-uniformities of temperature along the cross section of the fin is not justified in practical situations if the base temperature of the fin is considered uniform. Exception occurs for number values of Biot number less than 0.01.

In an analysis of any fin geometry, the constraints or assumptions are very important. Assumptions are employed to define and limit the problem and, of course, to simplify its solution. The most simplified constrains used are Murray (1938), Gardner (1945):
1 – The heat flow and temperature distribution throughout the fin are independent of time, i.e., the heat flow is steady.
2 – There are not heat sources in the fin itself.
3 –The heat flow to or the fin surface at any point is directly proportional to the temperature difference between the surface at that point and the surrounding fluid.
4 – The thermal conductivity of the fin is constant.
5 – The heat transfer coefficient is the same over the entire fin surface.
6 – The temperature of the surrounding fluid is uniform.
7 – The temperature of the base of the fin is uniform.
8 – The joint between the fin and the prime surface is assumed to offer no bond resistance.

Besides the analyses based on the foregoing simplify assumptions are not real-world analyses, design of heat transfer equipment utilizing extended surfaces is still based on the simplified constraints that employ the limiting assumptions and the Classical One-dimensional Radial Fin or Rectangular One-dimensional Fin.

II. Objective

Analytical solution of two-dimensional, steady-state heat conduction within extend rectangular surface is presented. In addition, the improved classical one-dimensional model is examined for these kinds of profile. The influence of governing parameters, Biot number and aspect ratio, is investigate and comparison is made with results of literature. The problem analyzed here is a particular case of the general solution presented by Cotta and Mikhailov (1997), and an application for an Electric Motor finned is presented, were the efficiency and efficacy are critically examined.

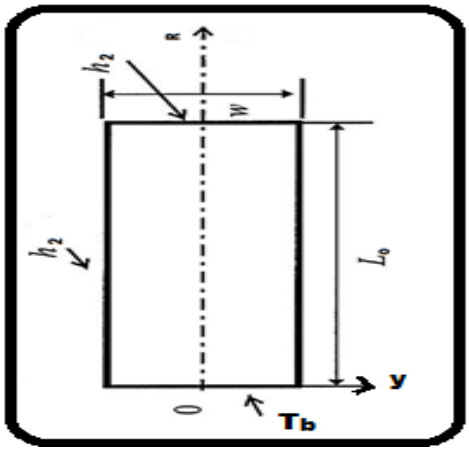

Figure 01 - Coordinates System and Geometric Parameters for Two-dimensional Rectangular Fin

III. METHODOLOGY

Consider the longitudinal fin of two-dimensional rectangular profile, subjected to a uniform base temperature.

The two-dimensional heat conduction equation is given, in dimensionless form:

$$\frac{\partial^2\theta(R,Y)}{\partial R^2} + K^2\frac{\partial^2\theta(R,Y)}{\partial Y^2} = 0 \ , 0 < R < 1 \ ; \ 0 < Y < 1 \qquad 01$$

with boundary conditions:

$$\theta(0,Y) = 1 \qquad 01.1$$

$$\frac{\partial\theta(1,Y)}{\partial R} + B_{i2}K\theta(1,Y) = 0 \ , \quad 0 < Y < 1 \qquad 01.2$$

$$\frac{\partial\theta(R,0)}{\partial Y} = 0 \qquad 01.3$$

$$\frac{\partial\theta(R,1)}{\partial Y} + B_{i2}K\theta(R,1) = 0 \ , \quad 0 < R < 1 \qquad 01.4$$

where the following dimensionless groups were employed:

$$\theta(R,Y) = \frac{T(r,y) - T_\infty}{T_b - T_\infty}; \ R = \frac{r}{L_o}; \ Y = \frac{y}{w/2}; \ K = \frac{L_o}{w/2}; \ B_{i2} = \frac{h_2(\frac{w}{2})}{k} \qquad 02$$

By separation of variables, we can have:

$$\theta(R,Y) = \sum_{m=1}^{\infty} \frac{sin\lambda_m cos\lambda_m Y}{\lambda_m + sin\lambda_m cos\lambda_m}\left[\frac{B_{i2}\sinh[\lambda_m K(1-R)] + \lambda_m\cosh[\lambda_m K(1-R)]}{B_{i2}\sinh[\lambda_m K] + \lambda_m\cosh[\lambda_m K]}\right] \qquad 03$$

where λ_m are the positive roots of the transcendental equation:

$$\lambda_m tan\lambda_m - B_{i2} = 0 \qquad 04$$

The average temperature at any cross-section along its length is then obtained from:

$$\theta_{Av}(R) = \int_0^1 \theta(R,Y)dY \qquad 05$$

$$\theta_{Av}(R) = 2\sum_{m=1}^{\infty} \frac{sin^2\lambda_m}{\lambda_m(\lambda_m + sin\lambda_m cos\lambda_m)} \left[\frac{B_{i2}\sinh[\lambda_m K(1-R)] + \lambda_m \cosh[\lambda_m K(1-R)]}{B_{i2}\sinh[\lambda_m K] + \lambda_m \cosh[\lambda_m K]}\right] \quad 06$$

The dimensionless heat transfer rate at the base, per unit length along the base then becomes:

$$Q_b = K\sqrt{B_{i2}} \sum_{m=1}^{\infty} \frac{sin^2\lambda_m}{(\lambda_m + sin\lambda_m cos\lambda_m)} \left[\frac{B_{i2}\cosh[\lambda_m K] + \lambda_m \sinh[\lambda_m K]}{B_{i2}\sinh[\lambda_m K] + \lambda_m \cosh[\lambda_m K]}\right] \quad 07$$

The efficiency is determinate by:

$$\eta = \frac{Q_b}{B_{i2}K(1+K)} \quad 08$$

and the effectiveness for:

$$\varepsilon = \frac{2Q_b}{B_{i2}K} \quad 09$$

The Classical One-dimensional Radial Fin problem is represented by the equation:

$$\frac{d^2\theta(R)}{dR^2} + \frac{1}{R}\frac{d\theta(R)}{dR} = B_{i2}K^2\theta(R) \quad 10$$

or

$$\frac{1}{R}\frac{d}{dR}\left[R\frac{d\theta(R)}{dR}\right] - B_{i2}K^2\theta(R) = 0 \quad 11$$

and the boundary conditions,

$$\theta(0) = 1 \quad 11.1$$

$$\frac{d\theta(1)}{dR} + B_{i2}K\theta(1) = 0 \quad 11.2$$

The problem of boundary conditions above is geometrically represented:

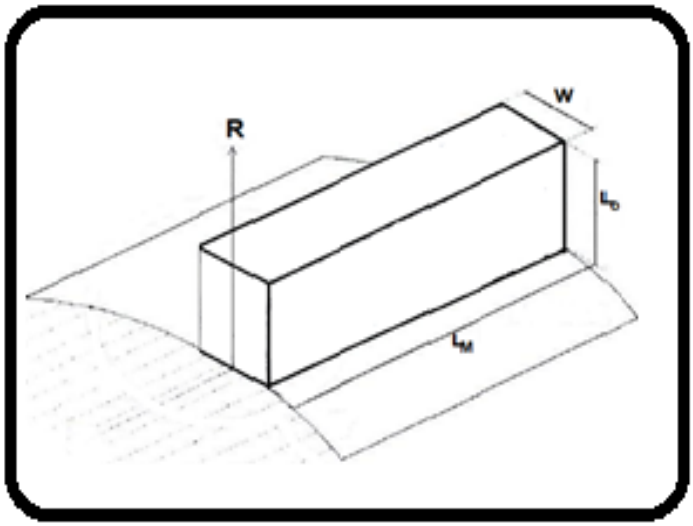

Figure 02 – Geometric Representation of Classical One-dimensional Radial Fin

The solution of Equation 10 is in the form

$$\theta(R) = C_1 \mathbb{I}_\nu(R) + C_2 \mathbb{K}_\nu(R) \quad 11.3$$

Where $\mathbb{I}_\nu$ and $\mathbb{K}_\nu$ are modified Bessel functions of order ν of the first and second kind respectively. The functions $\mathbb{I}_\nu(R)$ and $\mathbb{K}_\nu$ are two linearly independent solutions of Equation 10, and are valid for all values of ν. Figure 03 shows a plot of zero end first-order modified Bessel functions. It is be noted that $\mathbb{K}_\nu$ functions become infinite as R goes to zero, whereas $\mathbb{I}_\nu(R)$ functions become infinite as R goes to infinity.

The numerical values of modified Bessel functions of the first and second kind are given in Table 02, whit comparison of values given by Ösizik (1968) in Appendices III.

Can be proven Butkov (1978), Boyce & Diprima (1986), Hildebrand (1962)], the equation 10 is a special case of the modified Bessel equation, whose solution is given by Butkov (1978); Özisik (1968):

$$\theta_{Av}(R) = \frac{\{\mathbb{K}_0(\sqrt{B_{i2}^+}KR)[B_{i2}^+\mathbb{I}_0(\sqrt{B_{i2}^+}K) + \sqrt{B_{i2}^+}\mathbb{I}_1(\sqrt{B_{i2}^+}K)] - \mathbb{I}_0(\sqrt{B_{i2}^+}KR)[[B_{i2}^+\mathbb{K}_0(\sqrt{B_{i2}^+}K) - \sqrt{B_{i2}^+}\mathbb{K}_1(\sqrt{B_{i2}^+}K)]\}}{\{\mathbb{K}_0(\sqrt{B_{i2}^+}KR_b)[B_{i2}^+\mathbb{I}_0(\sqrt{B_{i2}^+}K) + \sqrt{B_{i2}^+}\mathbb{I}_1(\sqrt{B_{i2}^+}K)] - \mathbb{I}_0(\sqrt{B_{i2}^+}KR_b)[[B_{i2}^+\mathbb{K}_0(\sqrt{B_{i2}^+}K) - \sqrt{B_{i2}^+}\mathbb{K}_1(\sqrt{B_{i2}^+}K)]\}} \quad 12$$

and

$$Q_b = \frac{K}{4}\sqrt{B_{i2}^+}\frac{\{\mathbb{K}_1(\sqrt{B_{i2}^+}KR_b)[B_{i2}^+\mathbb{I}_0(\sqrt{B_{i2}^+}K) + \sqrt{B_{i2}^+}\mathbb{I}_1(\sqrt{B_{i2}^+}K)] + \mathbb{I}_1(\sqrt{B_{i2}^+}KR_b)[[B_{i2}^+\mathbb{K}_0(\sqrt{B_{i2}^+}K) - \sqrt{B_{i2}^+}\mathbb{K}_1(\sqrt{B_{i2}^+}K)]\}}{\{\mathbb{K}_0(\sqrt{B_{i2}^+}KR_b)[B_{i2}^+\mathbb{I}_0(\sqrt{B_{i2}^+}K) + \sqrt{B_{i2}^+}\mathbb{I}_1(\sqrt{B_{i2}^+}K)] - \mathbb{I}_0(\sqrt{B_{i2}^+}KR_b)[[B_{i2}^+\mathbb{K}_0(\sqrt{B_{i2}^+}K) - \sqrt{B_{i2}^+}\mathbb{K}_1(\sqrt{B_{i2}^+}K)]\}} \quad 13$$

where the improved solution, extending the range for the Biot number, is obtained with the following defined parameter Aparecido and Cotta (1988):

$$B_{i2}^+ = \frac{B_{i2}}{1.0 + \frac{B_{i2}}{4}} \quad 14$$

$$\eta = \frac{Q_b}{B_{i2}K^2} \quad 15$$

$\mathbb{K}_0$, $\mathbb{K}_1$, $\mathbb{I}_0$, $\mathbb{I}_1 are$modified Bessel functions of the first and second kind:

where,

$$\mathbb{I}_\mu(x) = \sum_{k=0}^{\infty} \frac{1}{k!\,\Gamma(\mu + k + 1)2^{\mu+2k}} x^{\mu+2k} \quad 16$$

and

$$\mathbb{K}_m(x) = \frac{(-1)^m}{2}\left[\frac{\partial \mathbb{I}_{-\mu}(x)}{\partial \mu} - \frac{\partial \mathbb{I}_\mu(x)}{\partial \mu}\right]_{\mu=m} \quad 17$$

For small R (Özisik):

$$\mathbb{I}_n(R) \cong \frac{1.0}{2^n n!}R^n \quad 18$$

$$\mathbb{K}_n(R) \cong -l_n R \;\; for\, n = 0 \;\; and\; \mathbb{K}_n(R) \cong \frac{2^{n-1}(n-1)!}{R^n} \;\; for \;\; n \neq 0 \quad 19$$

For $R \geq 10$ ($Özisik$):

$$\mathbb{I}_0(R) \cong \frac{0.3989e^R}{R^{\frac{1}{2}}}\left\{1+\frac{1}{8R}+\frac{9}{128R^2}+\frac{75}{1024R^3}\right\} \quad 20$$

$$\mathbb{I}_1(R) \cong \frac{0.3989e^{-R}}{R^{\frac{1}{2}}}\left\{1+\frac{3}{8R}-\frac{15}{128R^2}+\frac{105}{1024R^3}\right\} \quad 21$$

$$\mathbb{K}_0(R) \cong \frac{1.2533e^{-R}}{R^{\frac{1}{2}}}\left\{1-\frac{1}{8R}+\frac{9}{128R^2}-\frac{75}{1024R^3}\right\} \quad 22$$

$$\mathbb{K}_1(R) \cong \frac{1.2533e^{-R}}{R^{\frac{1}{2}}}\left\{1+\frac{3}{8R}-\frac{15}{128R^2}+\frac{105}{1024R^3}\right\} \quad 23$$

For large R (Özisik):

$$\mathbb{I}_n(R) \cong \frac{e^R}{\sqrt{2\pi R}} \quad 24$$

$$\mathbb{K}_n(R) \cong \sqrt{\frac{\pi}{2R}}e^{-R} \quad 25$$

Despite the relative simplicity of the equations approximated above, it is difficult to define the limits of application of each of them. A solution found to solve the problem of application ranges, and facilitate the use of modified Bessel Functions, was to implement polynomial interpolations that satisfy the equations within certain ranges of the variable, where,

IF (R.LT. 0.1d0) Then:

$$\begin{aligned}\mathbb{I}_0(R) = {} & 1.0d0 + (R/2.0d0) ** 2.0d0 + (R/2.0d0) ** 4.0d0/4.0d0 + (R/2.0d0) ** 6.0d0/36.0d0 \\ & + (R/2.0d0) ** 8.0d0/576.0d0 + (R/2.0d0) ** 10.0d0/1.44d4 + (R/2.0d0) * \\ & * 12.0d0/5.184d5 + (R/2.0d0) ** 14.d0/2.54012d5 + (R/2.d0) * \\ & * 16.d0/1.6257d7 \end{aligned} \quad 26$$

$$\begin{aligned}\mathbb{K}_0(R) = {} & -(Dlog(R/2.0d0) + Gama) * I0 + (R/2.d0) ** 2.d0 + (1.d0 + 1.d0/2.d0) \\ & * (R/2.d0) ** 4.d0/4.d0 + (1.d0 + 1.d0/2.d0 + 1.d0/3.d0) * (R/2.d0) * \\ & * 6.d0/36.d0 \end{aligned} \quad 27$$

$$\begin{aligned}\mathbb{I}_1(R) = {} & R/2.d0 + (R/2.d0) ** 3.d0/2.d0 + (R/2.d0) ** 5.d0/12.d0 + (R/2.d0) * \\ & * 7.d0/144.d0 + (R/2.d0) ** 9.d0/2.88d3 + (R/2.d0) * \\ & * 11.d0 \\ & /4.9766400d7 \end{aligned} \quad 28$$

$$\mathbb{K}_1(R) = 1.d0/R \quad 29$$

IF (R.GE.0.1d0.AND.R.LE.2.0d0) Then

$$\begin{aligned}\mathbb{K}_0(R) = {} & 3.192243447081073d0 - 9.075769668639543d0 * R + 13.60020730045569d0 * R * \\ & * 2.d0 - 11.71504474098401d0 * R ** 3.d0 + 5.871521019759846d0 * R * \\ & * 4.d0 - 1.684210215097076d0 * R ** 5.d0 + 0.2558084536798895d0 * R * \\ & * 6.d0 - 0.01593016574328118d0 * R * \\ & * 7.d0 \end{aligned} \quad 30$$

IF (R.GT.2.0d0.AND. R.LE.10.0d0) Then

$$\mathbb{K}_0(R) = 0.7821721640552073d0 - 0.7045671525518567d0 * R + 0.2803496848260917d0 * R ** 2.d0 - 0.06318534709170828d0 * R ** 3.d0 + 0.008638592898647074d0 * R ** 4.d0 - 0.0007120141578368239d0 * R * * 5.d0 + 3.261471310391972d - 5 * R ** 6.d0 - 6.385387558865935d - 7 * R ** 7.d0 \quad (31)$$

IF (R.GE.0.1d0.And.R.LE.1.0d0) Then

$$\mathbb{K}_1(R) = 30.1827605d0 - 346.7404234d0 * R + 1976.218928d0 * R ** 2.d0 - 6487.463063d0 * R ** 3.d0 + 13244.4264d0 * R ** 4.d0 - 17532.27536d0 * R ** 5.d0 + 15295.09625d0 * R ** 6.d0 - 8725.795328d0 * R ** 7.d0 + 3130.601004 * R ** 8.d0 - 640.6534448 * R ** 9.d0 + 57.00840557d0 * R * * 10.d0 \quad (32)$$

IF (R.GE.1.d0.AND. R.LE.2.0d0) Then

$$\mathbb{K}_1(R) = 6.481724834d0 - 17.8099371d0 * R + 23.52584122d0 * R ** 2.d0 - 17.73860386d0 * R ** 3.d0 + 7.937748727d0 * R ** 4.d0 - 2.078233527d0 * R ** 5.d0 + 0.2935162617d0 * R ** 6.d0 - 0.01724749822d0 * R * * 7.d0 \quad (33)$$

IF (R.GT.2.d0.AND. R.LE.6.0d0) Then

$$\mathbb{K}_1(R) = 1.838215305d0 - 2.210252282d0 * R + 1.209442242d0 * R ** 2.d0 - 0.3819367933d0 * R ** 3.d0 + 0.07395968326d0 * R ** 4.d0 - 0.00868374175d0 * R ** 5.d0 + 0.0005681634381d0 * R ** 6.d0 - 1.590421709d - 5 * R ** 7.d0 \quad (34)$$

IF (R.GT.6.d0.AND. R.LE.10.0d0) Then

$$\mathbb{K}_1(R) = 0.1533476443d0 - 0.08337728963d0 * R + 0.01838379927d0 * R ** 2.d0 - 0.002048103623d0 * R ** 3.d0 + 0.0001149941314d0 * R ** 4.d0 - 2.597769225d - 6 * R ** 5.d0 + 3.611891512d - 308 * R ** 6.d0 + 3.611833088d - 308 * R * * 7.d0 \quad (35)$$

IF (R.GE.0.1d0.AND. R.LE.3.8d0) Then

$$\mathbb{I}_0(R) = 0.9893575023d0 + 0.08480386797d0 * R + 0.06778775944d0 * R ** 2.d0 + 0.1590992556d0 * R ** 3.d0 - 0.04756769189d0 * R ** 4.d0 + 0.0106239223d0 * R ** 5.d0 + 3.611891541d - 308 * R ** 6.d0 + 3.611833088d - 308 * R * * 7.d0 \quad (36)$$

IF (R.GT.3.8d0.AND. R.LE.10.0d0) Then

$$\mathbb{I}_0(R) = -480.6699002d0 + 817.6684163d0 * R - 570.9865698d0 * R ** 2.d0 + 213.5897742d0 * R ** 3.d0 - 46.36731792d0 * R ** 4.d0 + 5.887386345d0 * R ** 5.d0 - 0.4076705361d0 * R ** 6.d0 + 0.01212271103d0 * R * * 7.d0 \quad (37)$$

IF (R.GE.0.1d0.AND. R.LE.4.0d0) Then

$$\mathbb{I}_1(R) = -0.01273191387d0 + 0.5907592411d0 * R - 0.172844278d0 * R ** 2.d0 + 0.2030581341d0 * R ** 3.d0 - 0.05259643127 * R ** 4.d0 + 0.01038926198d0 * R ** 5.d0 + 3.611891544d - 308 * R ** 6 + 3.611833088d - 308 * R * * 7.d0 \quad (38)$$

IF (R.GT.4.0d0.AND. R.LE.10d0) Then

$$\mathbb{I}_1(R) = -521.7686664d0 + 881.4602992d0 * R - 611.6718634d0 * R ** 2.d0 + 227.1939683d0 * R ** 3.d0 - 48.94559866d0 * R ** 4 + 6.162326128d0 * R ** 5.d0 - 0.4228027022d0 * R ** 6.d0 + 0.01243738144d0 * R * * 7.d0 \quad (39)$$

IV. RESULTS AND DISCUSSION

Below table of implemented six first eigenvalue of Equation 04, table and graphical implemented solution for Bessel modified functions:

Table 01 – Six First Eigenvalues of the Equation 04

B_{i2}	λ_1	λ_2	λ_3	λ_4	λ_5	λ_6
0.101	**0.3125**	**3.1734**	**6.2992**	**9.4354**	**12.5744**	**15.7143**
0.201	**0.4338**	**3.2042**	**6.315**	**9.446**	**12.5823**	**15.7207**
0.301	**0.5226**	**3.2344**	**6.3307**	**9.4566**	**12.5903**	**15.7271**
0.401	**0.5939**	**3.2638**	**6.3463**	**9.4671**	**12.5982**	**15.7334**
0.501	**0.6538**	**3.2926**	**6.3618**	**9.4776**	**12.6061**	**15.7398**
0.601	**0.7055**	**3.3206**	**6.3771**	**9.488**	**12.614**	**15.7461**
0.701	**0.751**	**3.348**	**6.3924**	**9.4984**	**12.6218**	**15.7524**
0.801	**0.7914**	**3.3746**	**6.4075**	**9.5088**	**12.6297**	**15.7587**
0.901	**0.8277**	**3.4006**	**6.4226**	**9.5191**	**12.6375**	**15.7650**

Table 02 – Implemented Bessel Modified Functions

X	K0(X)	K0(X)	I0(X)	I0(X)	K1(X)	K1(X)	I1(X)	I1(X)
1,00E-01	**2,427E+00**	2,426E+00	**1,003E+00**	1,003E+00	**9,854E+00**	1,000E+01	**5,010E-02**	5,000E-02
1,00E+00	**4,210E-01**	4,021E-01	**1,266E+00**	1,376E+00	**6,019E-01**	6,272E-01	**5,906E-01**	4,394E-01
2,00E+00	**1,139E-01**	1,135E-01	**2,280E+00**	2,270E+00	**1,399E-01**	1,404E-01	**1,591E+00**	1,606E+00
3,00E+00	**3,474E-02**	3,471E-02	**4,881E+00**	4,867E+00	**4,016E-02**	4,020E-02	**3,953E+00**	3,970E+00
4,00E+00	**1,116E-02**	1,116E-02	**1,130E+01**	1,129E+01	**1,248E-02**	1,249E-02	**9,760E+00**	9,771E+00
5,00E+00	**3,691E-03**	3,691E-03	**2,724E+01**	2,723E+01	**4,045E-03**	4,045E-03	**2,434E+01**	2,434E+01
6,00E+00	**1,244E-03**	1,244E-03	**6,723E+01**	6,722E+01	**1,344E-03**	1,344E-03	**6,134E+01**	6,135E+01
7,00E+00	**4,248E-04**	4,248E-04	**1,686E+02**	1,686E+02	**4,542E-04**	4,542E-04	**1,560E+02**	1,560E+02
8,00E+00	**1,465E-04**	1,465E-04	**4,276E+02**	4,275E+02	**1,554E-04**	1,554E-04	**3,999E+02**	3,999E+02
9,00E+00	**5,088E-05**	5,088E-05	**1,094E+03**	1,093E+03	**5,364E-05**	5,364E-05	**1,030E+03**	1,031E+03
9,90E+00	**1,975E-05**	1,975E-05	**2,561E+03**	2,561E+03	**2,072E-05**	2,072E-05	**2,428E+03**	2,428E+03

***Negrito**: M. Necati Özisik (1968)

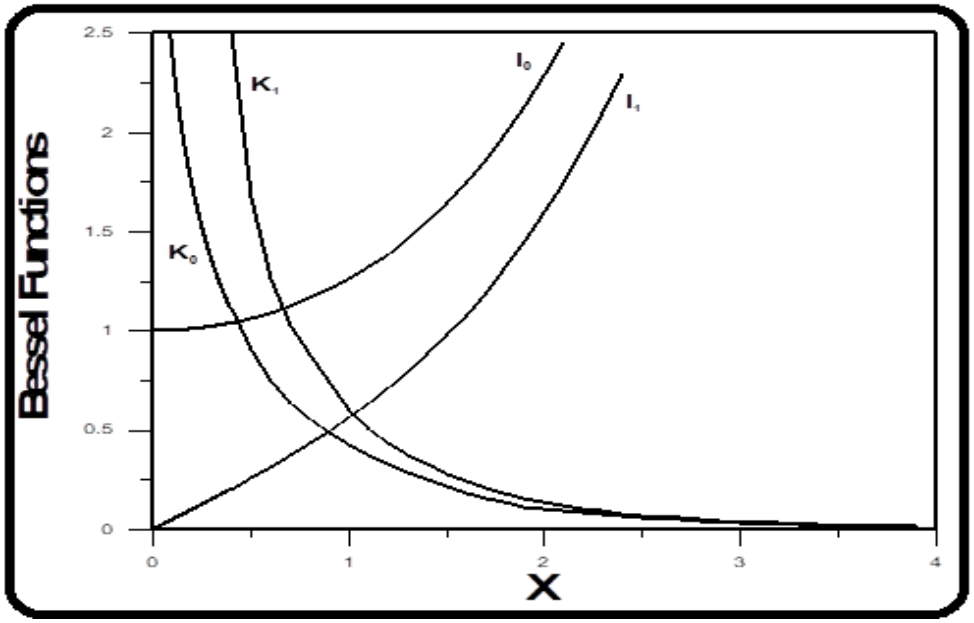

Figure 03 – Implemented Bessel Modified Functions

Figure 03 above presents the graphical solution implemented through polynomial interpolation. Continuity can be observed within all intervals for the preceding equations and they present the expected convergence and accuracy, as can be numerically attested by Table 02.

Table 03 – Comparative Results for Dimensionless Heat Transfer Rate

Bi	$\mathbb{K}$	Q_b^{RM} Cotta and Mikhailov (1977) – Table 4.3	(2.0 x Q_b^{EL}) /$\mathbb{K}$	Error	Error (%)	Q_b^{EL} Equation 07
0.01	**1.0**	**0.0395**	**0.0394**	**0.0001**	**0.2532**	**0.0196883**
0.01	**2.0**	**0.0582**	**0.0577**	**0.0005**	**0.8591**	**0.0576723**
0.01	**3.0**	**0.0759**	**0.0742**	**0.0017**	**2.2398**	**0.1113024**
0.01	**4.0**	**0.0923**	**0.0885**	**0.0038**	**5.2113**	**0.1769563**
0.01	**5.0**	**0.1072**	**0.0959**	**0.0113**	**10.5410**	**0.2397750**
0.10	**1.0**	**0.3547**	**0.3454**	**0.0093**	**2.6219**	**0.1727209**
0.10	**2.0**	**0.4631**	**0.4255**	**0.0376**	**8.1192**	**0.4255080**
0.10	**3.0**	**0.5319**	**0.4169**	**0.1194**	**17.8605**	**0.6553817**
0.10	**4.0**	**0.5726**	**0.4025**	**0.1701**	**29.7066**	**0.8050354**
0.10	**5.0**	**0.5956**	**0.3933**	**0.2023**	**33.9657**	**0.9832500**

Table 03 presents results for dimensionless heat transfer rate obtained by the author, Equation 07, and obtained by Cotta and Mikhailov (1997). Due to the different dimensioning performed, there was a need to transform the results through the expression Q_b =(2.0x$\boldsymbol{Q_b^{EL}}$) /$\mathbb{K}$. Cotta and Mikhailov advance the results until $\mathbb{K} = 5.0$. As a result, comparisons with higher values for aspect ratio were not possible.

Significant differences between models can be observed when the aspect factor is relatively high. In fact, in $\mathbb{K} = 5.0$ e Bi=0.10 the percentage error is of the order of 33%. It cannot be said that the difference occurs only in function of the transformation effected. It occurs, in fact, because in the model presented by Cotta and Mikhailov the dimensional factor used for the dimensionless rate is the perimeter associated with the base of the fin and not only the base of the fin, as occurs in the present model. We chose the base of the fin, w, as can be seen from Figure 01, since this dimensioning allows greater stability to the model and broadens the aspect ratio range to be analyzed, as can be seen from Figure 07 below.

Figures 04 and 05 present the average temperature profiles for two-dimensional and one-dimensional models, for different aspect ratio values and fixed Biot number. As can be observed, in both cases, for different values of Biot number, the average temperature at the top of the fin tends to the temperature of the medium as the aspect ratio grows.

Figure 06 displays the temperature profile at the top of the fin for two-dimensional model and different Biot number values. The effect of cross-heat exchange can be better observed for higher aspect ratio values. The highlighted frame presents the temperature profile for low value of the Biot number, 10-3, since the relative difference cannot be listed graphically in the previous scale (main chart).

Figure 07 shows the comparison between the one-dimensional and two-dimensional models for the dimensionless heat transfer rate, depending on the Biot number. For low aspect ratio value, K = 1, the results almost coincide. However, as the aspect ratio increases the coincidence, numeric, and graphics, it ceases to occur and the distance between the models extends significantly to higher values of the Biot number. There is also a qualitative difference between the results presented in the highest aspect ratio. The one-dimensional model responds late to the elevation of the fin height, and the two-dimensional model presents effects of cross-heat exchange for relatively low Biot numbers. It is possible to observe, for the two-dimensional model, which for high values of aspect ratio occurs a maximum in the heat exchange. This means that for higher values of Biot number it does not help to increase the height of the fin, as the heat exchange decreases rather than increase.

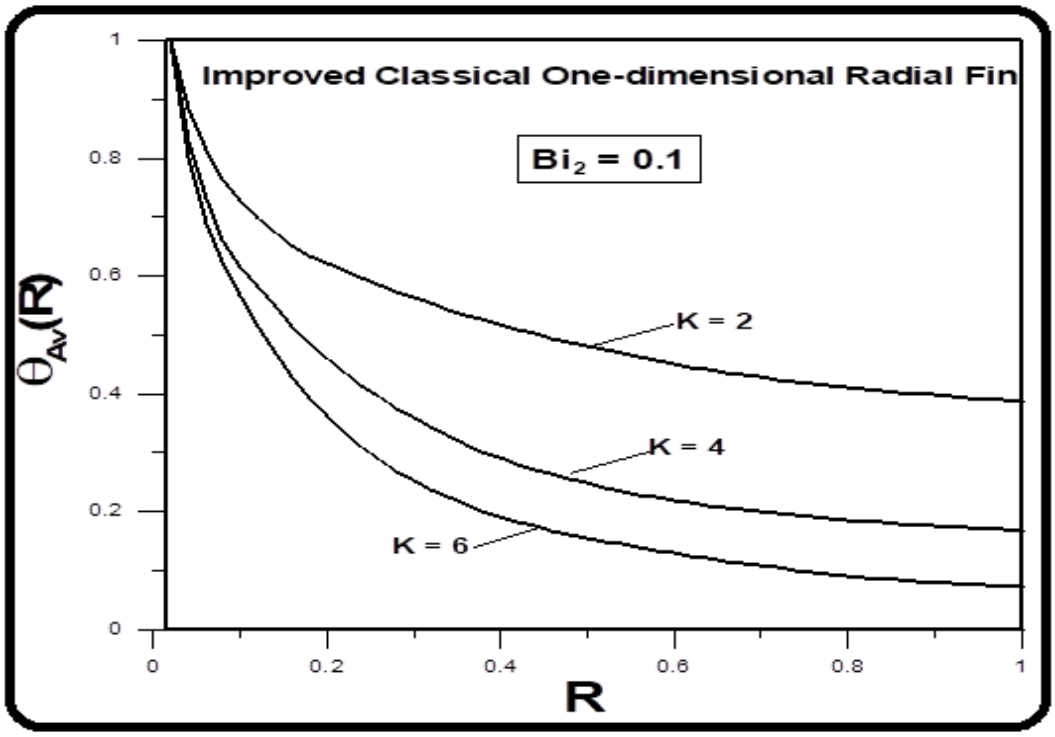

Figure 04 – Dimensionless Average Temperature for 1D Solution

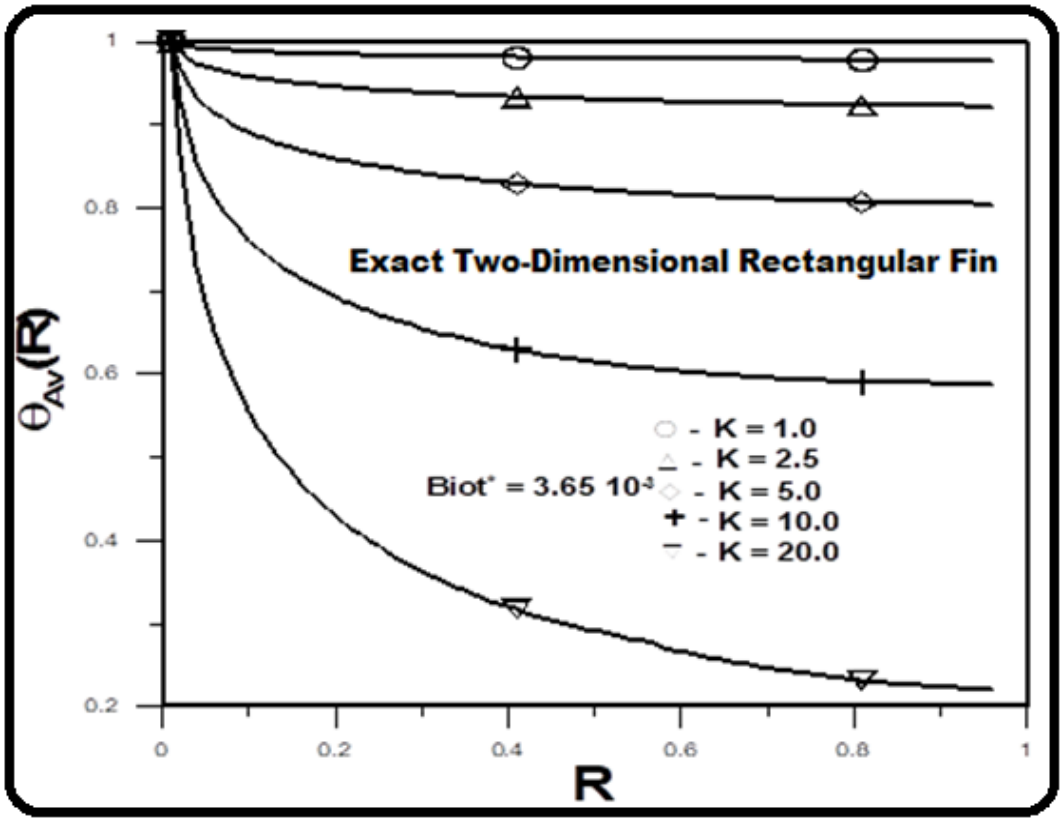

Figure 05 – Dimensionless Average Temperature for 2D Solution

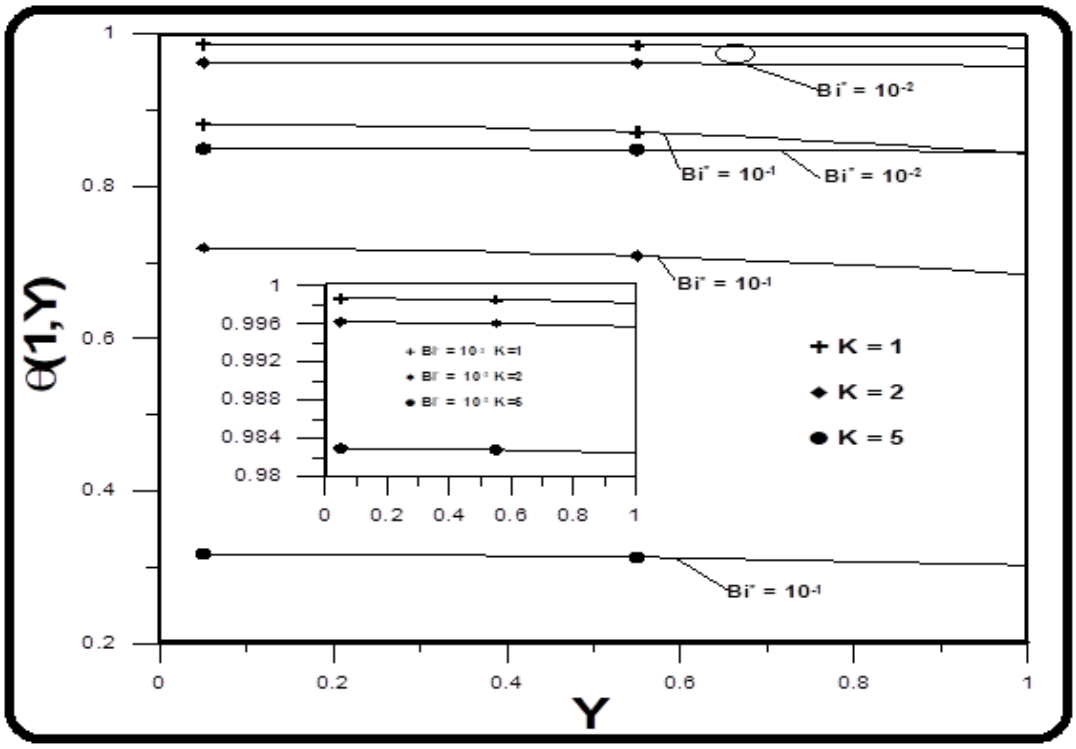

Figure 06 – Dimensionless Temperature on the Top of Fin for 2D Solution

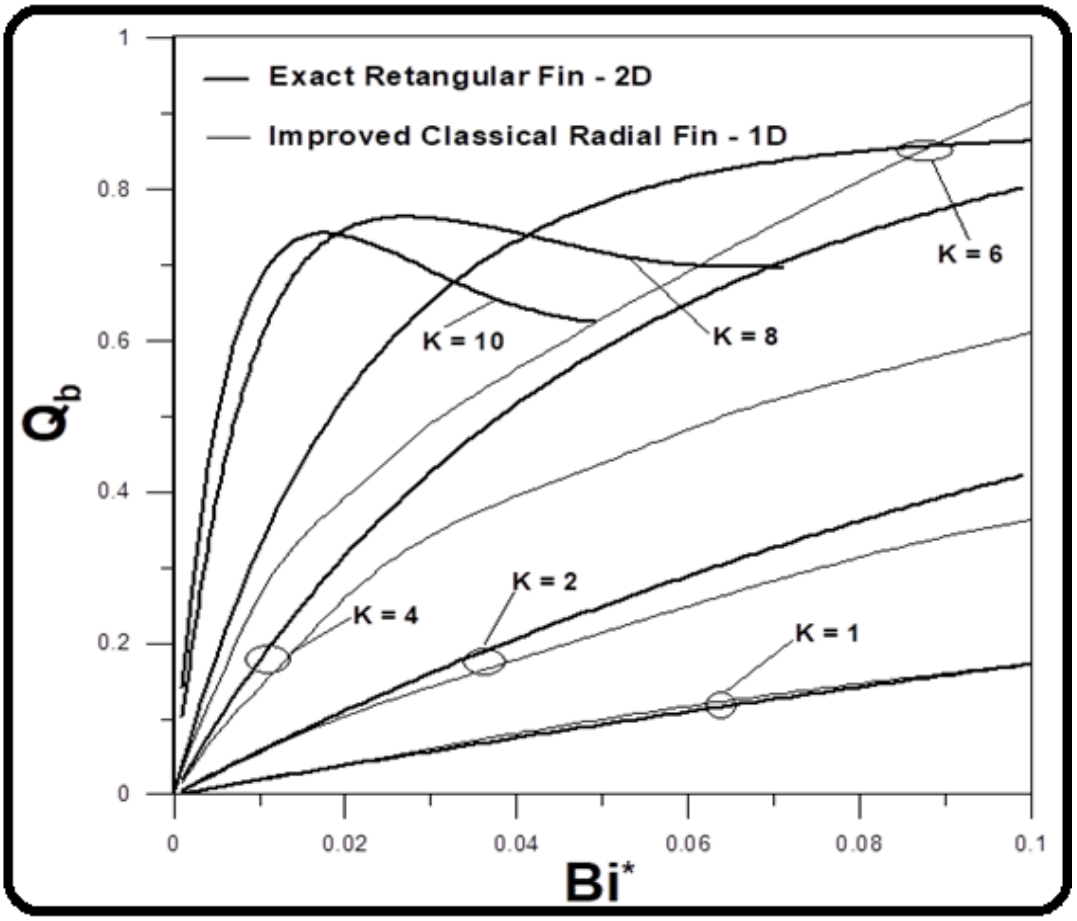

Figure 07 – Dimensionless Heat Transfer Rate at the Base of the Fin

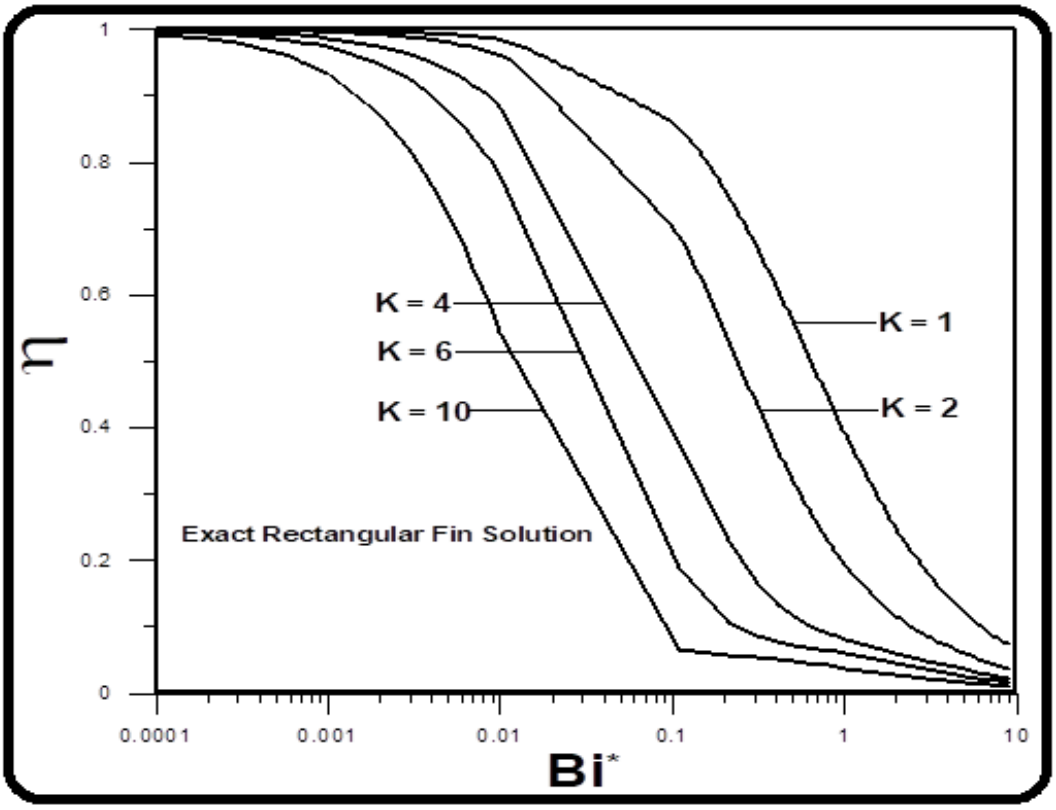

Figure 08 – Efficiency of the Fin

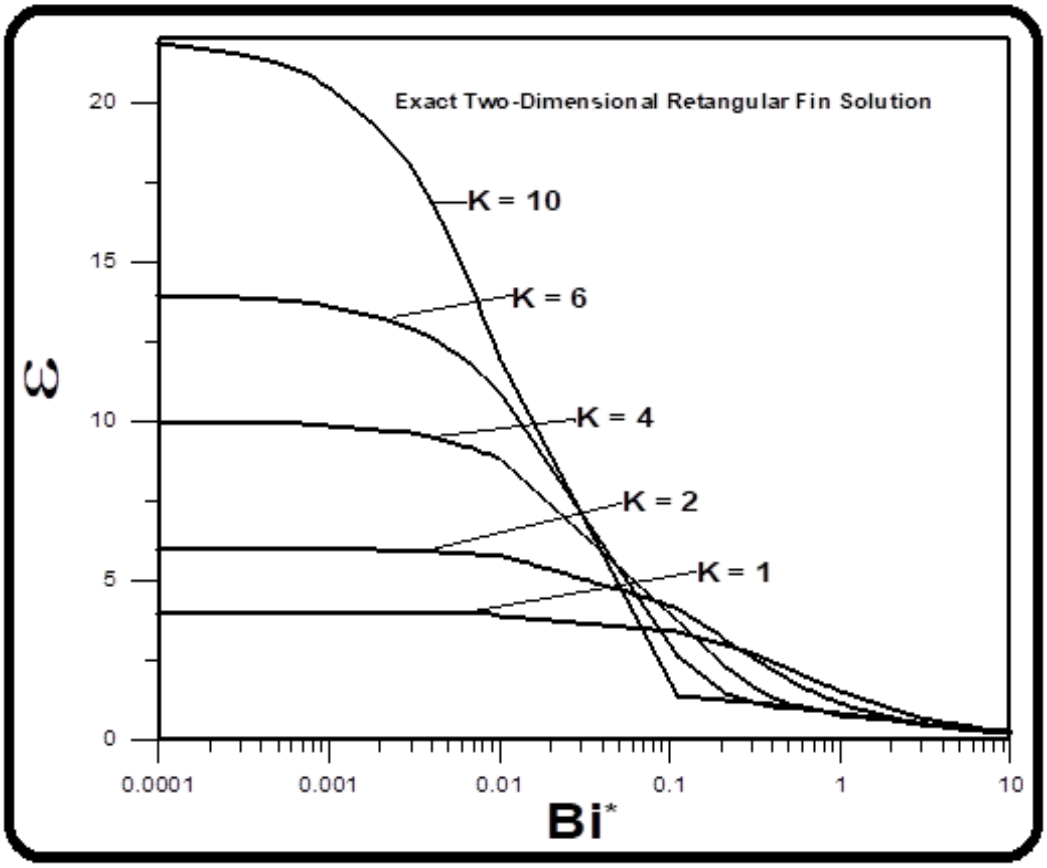

Figure 09 – Efficacy of the Fin

Figure 08 presents the results for efficiency depending on the Biot number and aspect factor as a parameter. Efficiency is high for low Biot number values and decreases when Biot increases. However, efficiency falls to the same Biot number when the aspect ratio increases. This can be explained by that as the fin increase, smaller is the temperature gradient for positions close to the top.

Figure 09 presents results for effectiveness as a function of Biot number, with aspect ratio as parameter. For smaller values of aspect ratio greater the range of application of the fin, in relation to the Biot number. When the aspect ratio increases, it increases effectiveness, but decreases the application range.

V. APPLICATION

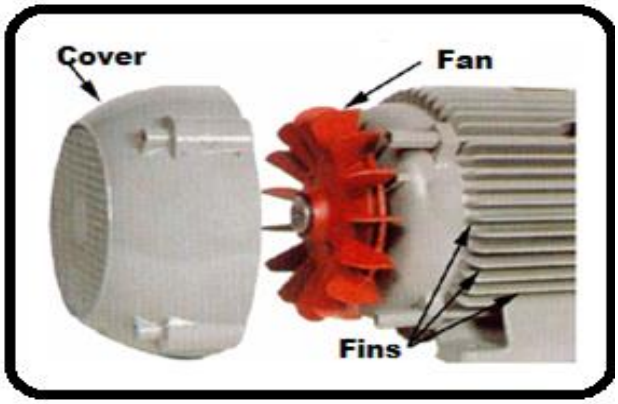

Figure 10 – Representation of an Electric Motor DC with Systems of Ventilation and Fin

An important industrial application of extended surfaces occurs in electric motors, as can be seen through Figure 10. Electric motors are of vital importance in the industry since they are used in

machines of all kinds, including, for example, in computer ventilation. A well-scaled fin and ventilation system can contribute to a significant economy of consumed energy. Recently, undergraduate works on these types of fins applications have been developed Tatiana (2017); Marcus Vinicius (2015); Ariane and Denise (2014); Yuri and Denise (2014). In fact, these studies presented the approximate one-dimensional and two-dimensional models, for rectangular profile fin, and explored several physical situations (prescribed temperature at the base; heat flux prescribed, including thermal resistance between the core and the motor housing), and under numerous environmental conditions (surrounding environment temperature). The data below, Table 04, refers to the quantities associated with fins and some operating conditions used in these studies.

Table 04 – Data for finned Electric Motor DC

Basic information for the fin system	
Engine width - L_M	**130,13 mm**
Width of fin base - w	**5,84 mm**
Fin height - L_o	**17,00 mm**
Conductivity - k	**80W/(m.K)**
Maximum base Temperature - T_b	**98ºC**
Maximum external Temperature - T_∞	**40ºC**

In this case, we have:

$$K = \frac{L_o}{w/2} = \frac{34.00}{5.84} \longrightarrow K = 5.82 \quad (40)$$

$$T_{Av}(R) = \theta_{Av}(R)(T_b - T_\infty) + T_\infty \longrightarrow T_{Av(R)} = 58.0\theta_{Av} + 48.0 \quad (41)$$

$$h_2 = \frac{kB_{i2}}{w/2} \longrightarrow h_2 = 27.40\,.10^3\,.\,B_{i2} \quad (42)$$

Table 05–Efficiency and Effectiveness of fin for K=5.84

B_{i2}	h_2 $W/(m^2K)$	η %	ε
10^{-3}	27.4	97,35	13,63
10^{-2}	274	77,17	10,91
10^{-1}	2740	18,80	2,63
10^{0}	27400	5,96	0,83
10^{1}	274000	1,52	0,21

Table 05 presents results for efficiency and effectiveness for the fin system of Figure 08, considering Biot number and aspect ratio. For relatively small values of Biot number the efficiency is high and the effectiveness justifies the placement of fins. The data show that in a range of heat transfer coefficient between 100 W/ (m^2.K) and 1500 W/(m^2.K) efficacy lies above 2.00. For Biot numbers above 0.1, there is definitely no justification for the use of the fin system, considering the used assumptions for the problem.

VI. CONCLUSIONS

The polynomial interpolation developed for Modified Bessel Functions helped implementation in all ranges of application, facilitating the use of them.

Temperature profiles for two-dimensional and one-dimensional models, for different aspect ratio values and fixed Biot number, was presented for comparison between these models. This comparison,

considering the dimensionless heat transfer rate, depending of the Biot number and aspect ratio, was made and the results demonstrate that:

01 - The effect of cross-heat exchange can be better observed for higher aspect ratio values.

02 - For low aspect ratio value, K = 1, the results almost coincide.

03 - As the aspect ratio increases the coincidence, numeric, and graphics, it ceases to occur and the numeric difference between the models extends significantly to higher values of the Biot number.

04 - There is also a qualitative difference between the results presented in the highest aspect ratio. The one-dimensional model responds late to the elevation of the fin height, and the two-dimensional model effects of cross-heat exchange, for relatively low Biot numbers, is appreciable.

05 - It is possible to observe, for the two-dimensional model, which for high values of aspect ratio occurs a maximum in the heat exchange. This means that for higher values of Biot number it does not help to increase the height of the fin, as the heat exchange decreases rather than increase.

Efficiency is high for low Biot number values and decreases when Biot increases. Efficiency falls to the same Biot number when the aspect ratio increases.

When the aspect ratio increases, it increases effectiveness, but decreases the application range.

About the Electric Motor used for example, the data show that, in a range of heat transfer coefficient between 100 W/ (M2. K) and approximately 1500 W/ (M2. K), efficacy lies above 2.00. For Biot numbers above 0.1, there is definitely no justification for the use of the fin system, considering the used assumptions for the problem.

VII. FUTURE WORK

As a suggestion for future work we recommend the application of the theory developed in finned compact heat exchangers, used in electronic systems and, for example, automotive radiators.

REFERENCES

[1]. George Oguntalaa, Gbeminiyi Sobamowob, Raed Abd-Alhameeda (2019) "Numerical analysis of transient response of convective-radiative cooling fin with convective tip under magnetic field for reliable thermal management of electronic systems"**.** Thermal Science and Engineering Progress 9 289–298.

[2]. Vitor Cunha Andrade (2018) "Performance Evaluation of a Quasi-Fractal Fin for Application on Aeronautic Thermal Dispensers". Course Completion Project presented to the Undergraduate Course in Aeronautical Engineering of the Federal University of Uberlândia, as part of the requirements to obtain the title of Bacharel in Aeronautic Engineering. Advisor: Dra. Priscila Ferreira Barbosa de Sousa.

[3]. Antonio Campo and Balaram Kundu (2017) "Exact Analytic Heat Transfer from an Annular Fin with Stepped Rectangular Profile". American Journal of Heat and Mass Transfer, Vol. 4 No. 4, pp. 146-155 doi:10.7726/ajhmt.2017.1013.

[4]. Tatiana de Almeida Mota Santos (2017**)** "Thermal Performance Analysis of Finned Electric Motors: Bidimensional Rectangular Fin Solution with Prescribed Base Temperature". Completion of course work. (Degree in Mechanical Engineering) - Oswaldo Aranha University Center - Volta Redonda. Advisor: Élcio Nogueira.

[5]. Karinate Valentine Okiy (2015) "An Assessment of Extended Surfaces Two-Dimensional Effects"**.** International Journal of Engineering Research in Africa Vol 15 pp 71-85.

[6]. Marcus Vinicius Ferreira Soares (2015**)** "Analysis of the influence of convection heat transfer coefficient on the temperature of the finned electric motor core with heat flow prescribed at the base"**.** Course Conclusion Paper. (Degree in Mechanical Engineering) - Volta Redonda University Center, Oswaldo Aranha Foundation. Advisor: Elcio Nogueira.

[7]. Hai-Ping Hu (2015) "The Two-Dimensional Heat Transfer Analysis in Arrayed Fins with the Thermal Dissipation Substrate"**.** Hindawi Publishing Corporation Mathematical Problems in Engineering Volume 2015, Article ID 716352, 9 pages http://dx.doi.org/10.1155/2015/716352

[8]. Novais, Ariane; Chagas, R. D. F.; NOGUEIRA, Élcio (2014) "Theoretical analysis of thermal performance of finned electric induction motors". Cadernos UniFOA (Online), v. IX, p. 19-34.

[9]. Yuri; Denise; Nogueira E. (2014) "Aluminum and cast iron in the production of finned electric motor carcasses: efficiency, costs, operational and environmental aspects". Cadernos UniFOA (Printed), v. IX, p. 11-19.

[10]. Denise; Novais, Ariane; E. Nogueira (2012) "Rectangular profile fin analytical solution: comparison of thermal performance between aluminum and cast iron in electric motors". Cadernos UniFOA (Printed), v. 20, p. 43.
[11]. A. D. Sommers and A. M. Jacobi (2006) "An Exact Solution to Steady Heat Conduction in a Two-Dimensional Annulus on a One-Dimensional Fin: Application to Frosted Heat Exchangers with Round Tubes"**.** Journal of Heat Transfer APRIL 2006, Vol. 128.
[12]. E.J. Corrêa, R.M. Cotta (1998) "Enhanced lumped-differential formulations of diffusion Problems"**.** Appl. Math. Modelling 22, 137±152.
[13]. R. M. Cotta and M. D. Mikhailov (1997) "Heat Conduction: Lumped Analysis, Integral Transforms, Symbolic Computation". J0hn Wiley & Sons, New York.
[14]. R.M. Cotta, R. Ramos (1993) "Error analysis and improved formulations for extended surfaces". Proceedings of the NATO - Advanced Study Institute on Cooling of Electronic Systems, NATO ASI Series E: Applied Sciences, vol.258, pp. 753±787.
[15]. A.D. KRAUS (1993) "Analysis of Extended Surface Arrays For Air-Cooled Electronic Equipment"**.** Advanced Study Institute on Cooling of Electronic Systems, NATO ASI Series E: Applied Sciences, vol.258.
[16]. S. OKTAY (1993) "Beyond Thermal Limits in Computer Systems Cooling"**.** Advanced Study Institute on Cooling of Electronic Systems, NATO ASI Series E: Applied Sciences, vol.258.
[17]. J. B. Aparecido and R. M. Cotta (1988) "Improved One-Dimensional Fin Solutions". Heat Transf. Eng., V. 11, no. 1, 49-59.
[18]. J.B. Aparecido, R.M. Cotta (1988) "Modified one-dimensional analysis of radial fins". Proceedings of the Second National Meeting of Thermal Sciences, ENCIT, pp. 225±228.
[19]. William E. Boyce and Richard C. Diprima (1986) "Elementary Differential Equations and Boundary Value Problems". John Willey & Sons, New York.
[20]. M. D. Mikhailov and M. N. Özisik (1984) "Unified Analysis and Solutions of Heat and Mass Diffusion". Dover Publications, INC., New York.
[21]. Eugene Butkov (1978) "Física Matemática". Guanabara Dois, Rio de Janeiro – RJ.
[22]. M. Necati Özisik (1968) "Boundary Value Problems of Heat Conduction". Dover Publications, INC., New York.
[23]. Juca, P. C. and Prata, A. T. "Heat Transfer on Finned Surfaces: Influence of Temperature Profile at Fin Base". ENCIT - National Meeting of Thermal Sciences.
[24]. Francis B. Hildebrand (1962) "Advanced Calculus for Applications". Prentice-Hall, INC. New Jersey.
[25]. Gardner, K. A. (1945) "Efficiency of extended surfaces". Transactions ASME, 67, 621–631.
[26]. Murray, W. M. (1938) "Heat dissipation through an annular disk or fin of uniform thickness". Transactions ASME, 60, A78–A88.

AUTHORS BIOGRAPHY

Élcio Nogueira http://lattes.cnpq.br/3470646755361575 Adjunct Professor, Faculty of Technology, State University of Rio de Janeiro - FAT / UERJ. He holds a degree in Physics from the Federal University of São Carlos - UFSCar (1981) with Extension in Nuclear Engineering (UFSCar), Specialization in Thermal Sciences from the Federal University of Viçosa - UFV (1985), Master in Aeronautical Mechanical Engineering by Instituto Tecnológico de Aeronautica - ITA (1988), PhD in Mechanical Engineering by the Federal University of Rio de Janeiro - UFRJ / COPPE (1993) and Post Doctorate in Thermal Sciences at the University of Miami - USA (1995). Research topics: Transport Phenomena, Mathematical and Computational Methods, Two-Phase Flow, Hypersonic Flow, Heat Transfer, Boundary Layer with application of Similarity Method.